

Quantum spin correlations through the superconducting-to-normal phase transition in electron-doped superconducting $\text{Pr}_{0.88}\text{LaCe}_{0.12}\text{CuO}_{4-\delta}$

Stephen D. Wilson*, Shiliang Li*, Jun Zhao*, Gang Mu†, Hai-Hu Wen†, Jeffrey W. Lynn‡, Paul G. Freeman§, Louis-Pierre Regnault¶, Klaus Habicht||, and Pengcheng Dai*,**††

*Department of Physics and Astronomy, University of Tennessee, Knoxville, TN 37996-1200; †National Laboratory for Superconductivity, Institute of Physics and National Laboratory for Condensed Matter Physics, Chinese Academy of Sciences, P.O. Box 603, Beijing 100080, China; ‡Center for Neutron Research, National Institute of Standards and Technology, Gaithersburg, MD 20899-6102; §Institut Laue-Langevin, 6, rue Jules Horowitz, BP156-38042 Grenoble Cedex 9, France; ¶Laboratoire de Magnétisme et Diffraction Neutronique, Service de Physique Statistique, Magnétisme et Supraconductivité, Département de Recherche Fondamentale sur la Matière Condensée, Commissariat à l'Énergie Atomique, 17 rue des Martyrs, 38054 Grenoble Cedex 9, France; ||Hahn-Meitner-Institut, Glienicke Strasse 100, D-14109 Berlin, Germany; and **Neutron Scattering Sciences Division, Oak Ridge National Laboratory, Oak Ridge, TN 37831-6399

Edited by Douglas J. Scalapino, University of California, Santa Barbara, CA, and approved July 26, 2007 (received for review May 24, 2007)

The quantum spin fluctuations of the $S = 1/2$ Cu ions are important in determining the physical properties of high-transition-temperature (high T_c) copper oxide superconductors, but their possible role in the electron pairing of superconductivity remains an open question. The principal feature of the spin fluctuations in optimally doped high- T_c superconductors is a well defined magnetic resonance whose energy (E_R) tracks T_c (as the composition is varied) and whose intensity develops like an order parameter in the superconducting state. We show that the suppression of superconductivity and its associated condensation energy by a magnetic field in the electron-doped high- T_c superconductor $\text{Pr}_{0.88}\text{LaCe}_{0.12}\text{CuO}_{4-\delta}$ ($T_c = 24$ K), is accompanied by the complete suppression of the resonance and the concomitant emergence of static antiferromagnetic order. Our results demonstrate that the resonance is intimately related to the superconducting condensation energy, and thus suggest that it plays a role in the electron pairing and superconductivity.

spin fluctuations | strongly correlated electron materials | superconductivity

The parent compounds of the high- T_c copper oxide superconductors are Mott insulators characterized by a very strong antiferromagnetic (AF) exchange in the CuO_2 planes and static long-range AF order. Doping holes or electrons into the CuO_2 planes suppresses the static AF order and induces a superconducting phase, with energetic short-range AF spin fluctuations that are peaked around the AF wave vector $\mathbf{Q} = (1/2, 1/2)$ in the reciprocal space of the two-dimensional CuO_2 planes (Fig. 1*a*) (1). Understanding the relationship between the insulating AF and superconducting phases remains a key challenge in the search for a microscopic mechanism of high- T_c superconductivity (2, 3). For optimally hole- and electron-doped high- T_c superconductors, the most prominent new feature in the spin fluctuation spectrum is a collective magnetic excitation known as the resonance mode, which also is centered at $\mathbf{Q} = (1/2, 1/2)$ and whose characteristic energy (E_R) is proportional to T_c (4–8). The resonance only appears below the superconducting transition temperature in these optimally doped systems and is fundamentally linked to the superconducting phase itself.

The resonance previously has been suggested as contributing a major part of the superconducting condensation (9), measuring directly the condensation fraction (10), and possessing enough magnetic exchange energy to provide the driving force for high- T_c superconductivity (11–13), but its small spectral weight compared with spin waves in the AF insulating phase may disqualify the mode from these proposed roles (14). One way to determine the microscopic origin of the resonance is to test its relationship to the superconducting condensation energy.

Strictly speaking, the notion of superconducting condensation energy is an ill-defined concept if the normal state fluctuation effects are important as in the case of hole-doped high- T_c copper oxides (15, 16). However, in the absence of an accepted microscopic theory, one may still use the mean-field expression to estimate the condensation energy to determine whether the mode can indeed contribute to the interaction necessary for electron pairing and superconductivity (14). Within the t - J model, a direct determination of the magnetic exchange energy available to the superconducting condensation energy requires the knowledge of the wave vector and energy dependence of the normal-state spin excitations at zero temperature (17), a quantity that has not been possible to obtain due to the presence of superconductivity. In principle, this can be rectified by studying the evolution of the zero (low) temperature spin excitations through the superconducting-to-normal state phase transition using magnetic field as a tuning parameter. Unfortunately, the large upper critical fields ($H_{c2} > 30$ T) required to completely suppress superconductivity in optimally hole-doped superconductors prohibit the use of neutron scattering in such a determination. In the lower field measurements on $\text{La}_{2-x}\text{Sr}_x\text{CuO}_4$, neutron scattering experiments have found that a magnetic field causes intensity to shift into the zero-field spin gap at the expense of the resonance (18, 19), which is consistent with the idea that the resonance is being gradually pushed into the elastic channel where a quantum critical point separates the superconducting state from an AF state (20, 21). Raman scattering results, however, showed that the primary effect of an applied field is simply to increase the volume fraction of the AF phase at the expense of the superconducting phase, thus suggesting an intrinsic electronic phase separation of these two phases (22).

Electron-doped superconductors require a much lower upper critical field ($H_{c2} < 10$ T) to completely suppress superconductivity (23), thereby enabling one to probe the evolution of the spin excitations, resonance, and static AF order in these materials as the system is transformed from the superconducting state

Author contributions: S.D.W. and P.D. designed research; S.D.W., S.L., J.Z., G.M., H.-H.W., J.W.L., P.G.F., L.-P.R., K.H., and P.D. performed research; S.D.W. analyzed data; and S.D.W., H.-H.W., J.W.L., and P.D. wrote the paper.

The authors declare no conflict of interest.

This article is a PNAS Direct Submission.

Abbreviations: AF, antiferromagnetic; PLCCO, $\text{Pr}_{0.88}\text{LaCe}_{0.12}\text{CuO}_{4-\delta}$; CEF, crystalline electric field.

††To whom correspondence should be addressed. E-mail: daip@ornl.gov.

This article contains supporting information online at www.pnas.org/cgi/content/full/0704822104/DC1.

© 2007 by The National Academy of Sciences of the USA

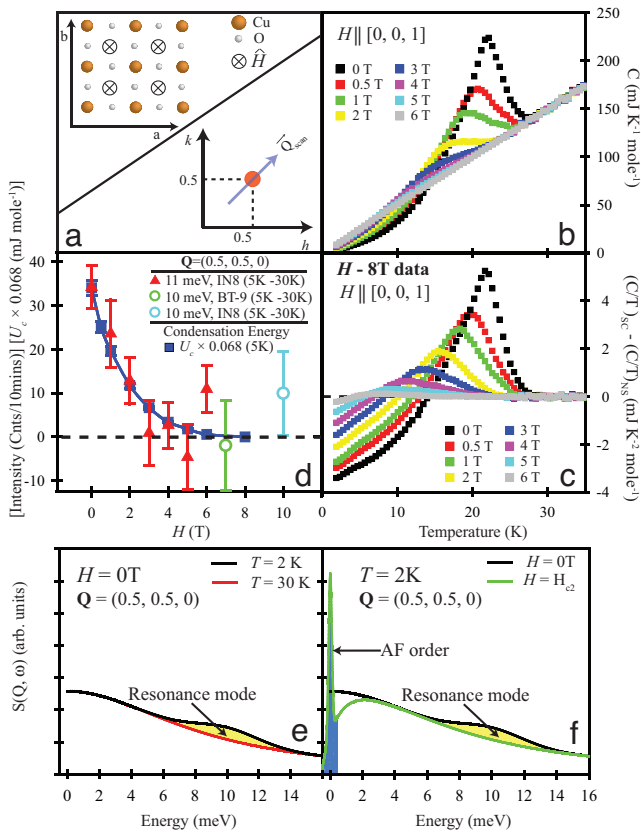


Fig. 1. Specific heat measurements of the superconducting condensation energy and summary of neutron scattering results for PLCCO ($T_c = 24$ K). (a) (Upper) The two-dimensional CuO_2 plane. (Lower) Schematic of typical constant-energy scans through reciprocal space. Spin excitations are centered at $\mathbf{Q} = (1/2, 1/2, 0)$. (b) Field dependence of the total electronic specific heat versus temperature. Data taken at 8 T were established to be above H_{c2} (25) and were used to isolate and subtract background contributions from the normal-state phonon/electronic heat capacity. To obtain the normal-state electronic specific heat γT , 8-T data were fitted by $C = \gamma T + \beta T^3$, where βT^3 is the phonon contribution. The resulting linear electronic contribution γT ($\gamma = 5$) was added back to the field-subtracted data to obtain the total electronic specific heat. (c) Field-subtracted measurements of the specific heat $(C_{SC} - C_N)/T$ versus temperature. The resulting entropy loss $S_N(T) - S_{SC}(T) = \int_0^T (C_N - C_{SC})dT/T'$ can then be calculated. (d) Condensation energy, U_c , determined from Eq. 1 and plotted as solid blue square symbols connected by a solid line. Intensity of the resonance mode plotted as a function of applied field. Red triangles denote peak intensity measurements at $\mathbf{Q} = (1/2, 1/2, 0)$, $\hbar\omega = 11$ meV at $T = 4$ K with the normal state background at $T = 30$ K subtracted. For field strengths of >6 T, entire \mathbf{Q} scans were performed to resolve the resonance excitation. The 5 K – 30 K peak intensities of \mathbf{Q} scans at 6.8 T and 10 T taken from Gaussian fits on a linear background (whose raw data are shown in Fig. 2) are plotted as open green (6.8 T) and teal circles (10 T). (e) Schematic plots of the zero-field $S(\mathbf{Q}, \omega)$ at $\mathbf{Q} = (1/2, 1/2, 0)$ below and above T_c . (f) For $H > H_{c2}$, the complete suppression of the resonance mode is observed along with the simultaneous appearance of a static AF order.

into the normal state at low temperature. Here we present electronic specific heat, elastic and inelastic neutron scattering results on the optimally electron-doped superconductor $\text{Pr}_{0.88}\text{LaCe}_{0.12}\text{CuO}_{4-\delta}$ (PLCCO) ($T_c = 24$ K) (8). We show that a magnetic field that suppresses the superconducting condensation energy in PLCCO also suppresses the resonance in a remarkably similar way (Fig. 1d). Furthermore, the reduction in magnetic scattering at the resonance energy with increasing magnetic field is compensated by the intensity gain of the elastic scattering at the AF ordering wave vector $\mathbf{Q} = (1/2, 1/2, 0)$ (Fig. 1e and f). Therefore, the superconducting phase without static

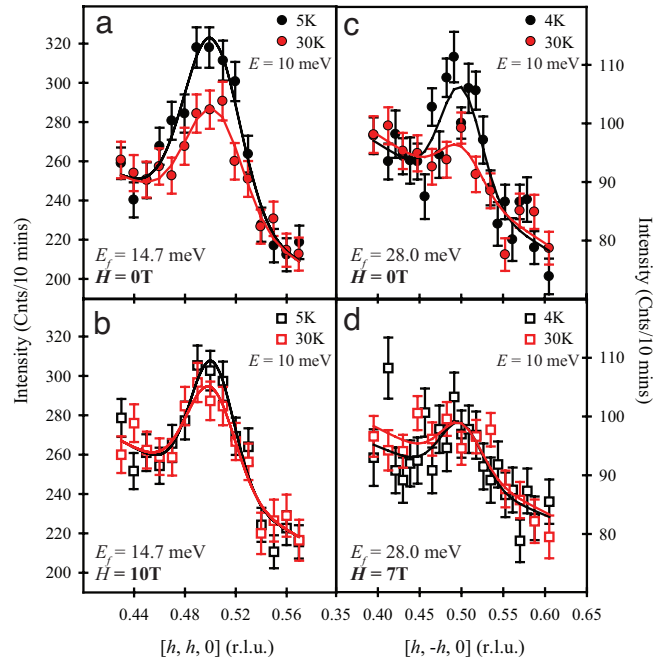


Fig. 2. Inelastic neutron measurements showing the suppression of the resonance mode under a c -axis-aligned magnetic field. (a) Zero field \mathbf{Q} scans at $\hbar\omega = 10$ meV at 5 K and 30 K on IN-8 with 60° - 60° - 5 - 60° -open collimations with neutron final energy fixed at $E_f = 14.7$ meV. The spectral weight increase below T_c demonstrates the presence of the resonance mode. (b) Ten-tesla \mathbf{Q} scans at $\hbar\omega = 10$ meV again on IN-8 showing no difference between the 5-K and 30-K intensities. Throughout our experiments, magnetic fields are always applied above 30 K and the samples were field-cooled to low temperature. (c) \mathbf{Q} scans on BT-9 with 40° - 48° - 5 - 40° - 80° collimations showing the resonance intensity again at 10 meV in 0 T using $E_f = 28$ meV. (d) Identical \mathbf{Q} scans at 5 K and 30 K showing the disappearance of the resonance mode under 6.8 T.

AF order can be directly transformed into an ordered AF phase without superconductivity in electron-doped PLCCO via the application of a magnetic field. These results present the possibility that the resonance is intimately related to electron pairing and superconductivity.

Results and Discussion

We used inelastic neutron scattering experiments on the IN-8, IN22, BT-9, and V2 triple-axis spectrometers to map out the field dependence of the magnetic scattering function, $S(\mathbf{Q}, \omega)$, over a range of energies ($0 \leq \hbar\omega \leq 18$ meV) in electron-doped PLCCO. We chose to study PLCCO because the crystalline electric field (CEF) ground state of Pr^{3+} in PLCCO is a nonmagnetic singlet and Ce^{4+} is nonmagnetic (24), thus greatly simplifying the interpretation of the data. Additionally, as will be discussed later, nearly optimally doped PLCCO ($T_c = 24$ K) has an experimentally determined and easily accessible upper critical field, $H_{c2} = 7$ T (Fig. 1b), necessary for the complete suppression of the superconducting phase (25).

Because previous work on hole-doped superconducting $\text{YBa}_2\text{Cu}_3\text{O}_{6.6}$ showed that a moderate c -axis-aligned magnetic field can suppress the intensity of the resonance (12), we first probed the influence of such a field on the recently discovered resonance in electron-doped PLCCO (8). Fig. 2a and c show \mathbf{Q} scans through $(1/2, 1/2, 0)$ at the resonance energy ($E_R \approx 10$ meV) in zero field on the IN-8 and BT-9 triple-axis spectrometers, respectively. Consistent with an earlier observation (8) and the new polarized neutron beam measurements [see supporting information (SI) Appendix], cooling from the normal ($T = T_c + 6$ K) to the superconducting ($T \approx T_c - 20$ K) state clearly

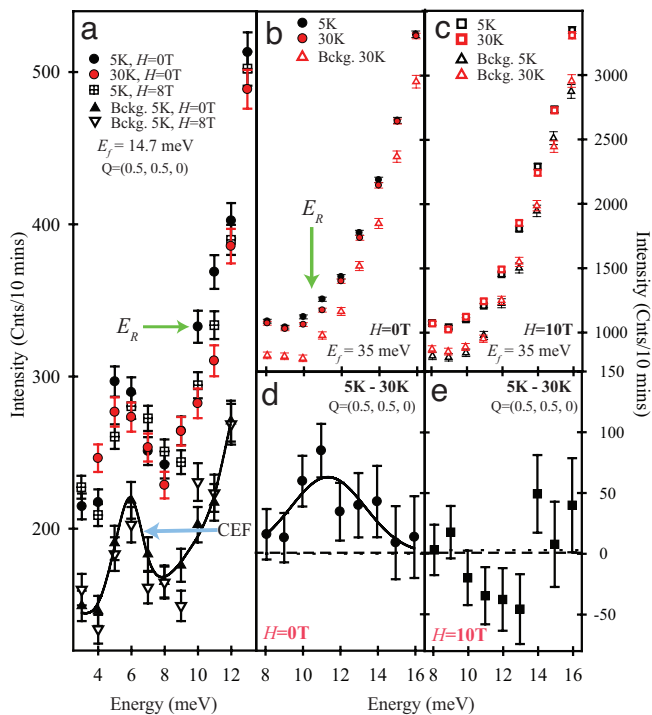


Fig. 3. Inelastic neutron measurements of magnetic field effect on the energy dependence of the spin fluctuations in PLCCO ($T_c = 24$ K). (a) Energy scans at $(1/2, 1/2, 0)$ taken on IN-8 at both 5 K and 30 K in 0 T and 8 T. The data show a clear suppression in 5-K scattering intensity at the resonance energy, E_R , under an 8-T field. Background points were collected at $\mathbf{Q} = (0.6, 0.6, 0)$. The 6-meV peak originates from a CEF excitation (8). (b) Energy scans at 5 K and 30 K at $(1/2, 1/2, 0)$ in 0 T on IN-8. Background data at $(0.6, 0.6, 0)$ and 30 K also are plotted. (c) Energy scans at 5 K and 30 K at $(1/2, 1/2, 0)$ in 10 T on IN-8. Background data were collected at $(0.6, 0.6, 0)$ at both 5 K and 30 K. (d and e) Temperature-subtracted (5 K – 30 K) energy scans collected at $(1/2, 1/2, 0)$ under 0 T and 10 T, respectively. The energy-integrated intensity from 8 to 16 meV is 314 ± 77 counts in 10 min at 0 T and -19 ± 85 counts in 10 min at 10 T.

enhances the magnetic scattering at $(1/2, 1/2, 0)$, which we define as the resonance (Fig. 1e). After applying a field greater than ($H = 10$ T) or near ($H = 7$ T) H_{c2} , these same \mathbf{Q} scans show that the superconductivity-induced enhancement (the resonance) in zero field (Fig. 2 a and c) has now been completely suppressed, leading only to normal state AF spin fluctuations (Fig. 2 b and d). Because the Pr^{3+} CEF excitations are weakly wave-vector-dependent (24), the magnetic field-induced suppression at $\mathbf{Q} = (1/2, 1/2, 0)$ must arise from the reduction of Cu^{2+} spin fluctuations at the resonance energy.

Fig. 3 summarizes the energy dependence of the scattering obtained on IN-8 at the peak center [$\mathbf{Q} = (1/2, 1/2, 0)$] and background [$\mathbf{Q} = (0.6, 0.6, 0)$] positions (Figs. 1a and 2b) for temperatures below and above T_c (i.e., 5 K and 30 K) and under zero, 8-T, and 10-T fields. Turning first to data collected by using a neutron final energy of $E_f = 14.7$ meV (Fig. 3a), the results at zero field are consistent with earlier measurements (see figure 3 in ref. 8) and show enhanced magnetic scattering at ≈ 10 meV below T_c , indicative of the resonance. Our polarized neutron beam measurements confirmed the magnetic nature of the mode (see SI Appendix). A Pr^{3+} CEF excitation at $\hbar\omega = 6$ meV also is observed in both signal and background scans (8). Although application of an 8-T magnetic field has no influence on the nonmagnetic background and the 6 meV CEF excitation at 5 K, there is a clear suppression of scattering at the resonance energy of 10 meV at 5 K (Fig. 3a). To cover a wider energy range around 10 meV at $\mathbf{Q} = (1/2, 1/2, 0)$, we carried out measurements using

$E_f = 35.0$ meV (Fig. 3 b and c). In the zero field case, the temperature difference data (Fig. 3d) again show a clear resonance peak at 11 meV, identical to the results of polarized neutron beam measurements (see SI Appendix). However, this well defined resonance peak vanishes when a 10-T field is applied, as confirmed by comparing the energy-integrated (from 8 to 16 meV), superconductivity-induced intensity changes between zero (314 ± 77 counts in 10 min) (Fig. 3d) and 10 T (-19 ± 85 counts in 10 min) (Fig. 3e). Future experiments at lower fields are necessary to determine whether the suppression observed in the \mathbf{Q} scans shown in Fig. 2 is due to a downward shifting of the mode's energy with increasing field, as seen in hole-doped $\text{La}_{2-x}\text{Sr}_x\text{CuO}_4$ (18, 19).

To probe the field-suppressed spectral weight distribution of the resonance, we have carried out systematic elastic scattering measurements across $\mathbf{Q} = (1/2, 1/2, 0)$ under various magnetic fields. Although previous muon spin relaxation measurements have observed the emergence of field-induced AF order throughout the volume of optimally doped PLCCO (26), neutron diffraction experiments have failed, possibly because of insufficient sample volume, to detect such a signal for optimally and overly doped PLCCO (27, 28). Because our PLCCO samples have no observable static AF order above $T = 0.6$ K (8), we would expect the observed peak at $(1/2, 1/2, 0)$ in Fig. 4b to be nonmagnetic and thus weakly temperature-dependent, which is indeed the case, as shown in scattering profiles between 2 K and 30 K (Fig. 4b). However, when an 8 T c -axis-aligned magnetic field is applied, field-induced magnetic intensity appears at the $\mathbf{Q} = (1/2, 1/2, 0)$ position (Fig. 4a). The field subtraction (8 T – 0 T) data at $T = 2$ K in Fig. 4c show this induced order without the presence of the residual nonmagnetic structural peak at $(1/2, 1/2, 0)$. The temperature dependence of the scattering reveals that the AF field-induced order increases with decreasing temperature (Fig. 4g), remarkably similar to the field-induced incommensurate elastic scattering from hole-doped $\text{La}_{1.9}\text{Sr}_{0.1}\text{CuO}_4$ (29) and $\text{La}_2\text{CuO}_{4+y}$ (30).

To demonstrate that the field-induced effect observed in Fig. 4c is indeed related to the suppression of superconductivity, we note that H_{c2} in copper oxides are highly anisotropic with respect to the direction of an applied field. Whereas a c -axis-aligned field can suppress superconductivity most efficiently, the same field parallel to the CuO_2 planes would have a substantially reduced effect on superconductivity. On the contrary, however, magnetic signal resulting from a simple polarization of paramagnetic Pr^{3+} moments in PLCCO is smaller for fields along the c -axis compared with that in the ab -plane (see SI Appendix). Fig. 4d shows \mathbf{Q} scans through $(1/2, 1/2, 0)$ on an identical PLCCO ($T_c = 24$ K) sample aligned in the $[h, h, l]$ zone such that the vertical field ($H \approx 6.8$ T) was applied along the in-plane wave vector $[-1, 1, 0]$ direction. The field subtraction results (Fig. 4e) indicate that there is no observable induced magnetic signal at 2 K. Now, realigning the same crystal in the $[h, k, 0]$ zone on the same spectrometer with the same magnet, the field subtraction results reveal a clear induced peak at $(1/2, 1/2, 0)$ (Fig. 4f). This is direct and unambiguous evidence that the field effect in PLCCO is associated with the suppression of superconductivity.

Fig. 4h shows that the induced order increases approximately linearly with increasing field up to H_{c2} . The appearance of the field-induced order is remarkably similar to the induced static moment seen in $\text{La}_{1.856}\text{Sr}_{0.144}\text{CuO}_4$ (31), which is thought to be near a quantum critical point between the “mixed phase” (where the superconducting and AF phases coexist) and the phase-pure superconducting phase (20, 21). Because both hole-doped $\text{La}_{1.856}\text{Sr}_{0.144}\text{CuO}_4$ (31) and electron-doped PLCCO ($T_c = 24$ K) (8) have no static AF order at zero field, field-induced AF order cannot be due to modifications of residual AF order. With the present data, however, it is difficult to decipher any lower critical field threshold necessary for the emergence of static AF order in

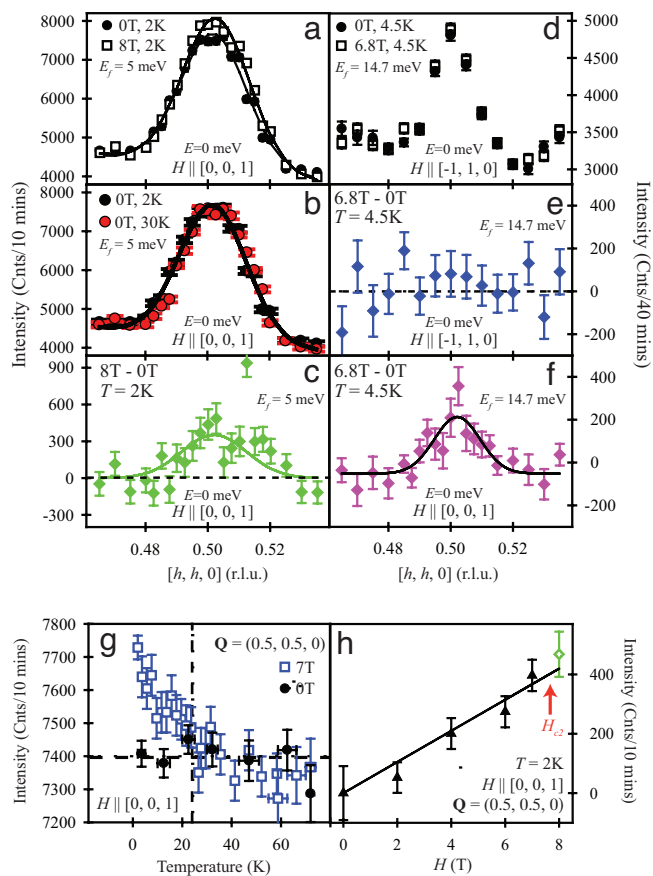


Fig. 4. Elastic neutron data demonstrating field-induced AF order under a c-axis-aligned magnetic field in PLCCO ($T_c = 24$ K). (a) Elastic Q scans through $(1/2, 1/2, 0)$ in 0 T and 8 T at 2 K. Fits to the data are Gaussian line shapes on a linear background. Data were collected on V2 using 60°-open-S-open-collimations and $E_f = 5$ meV with a cold Be filter before the analyzer. (b) Elastic Q scans under 0 T at 2 K and 30 K. (c) $T = 2$ K field (8 T - 0 T) subtraction of data shown originally in a. (d) Low-T elastic Q scans through $(1/2, 1/2, 0)$ under 0 T and 6.8 T fields along the $[-1, 1, 0]$ direction (in the CuO_2 planes). Data were collected on BT-9 with 40°-48°-54°-80° collimations and 3 pyrolytic graphite filters. (e) Field subtraction (6.8 T - 0 T) data with $H \parallel [-1, 1, 0]$ as shown in d. (f) Identical field subtraction (6.8 T - 0 T) data with $H \parallel [0, 0, 1]$. (g) Temperature dependence of elastic intensity under both 0 T and 7 T. T_c is denoted by the vertical dashed line, and a fitted constant value for the 0 T intensity is shown as a dashed horizontal line. (h) Field dependence of peak intensity values measured at 2 K and $Q = (1/2, 1/2, 0)$, $\hbar\omega = 0$ meV with 0 T, 30 K measured background value subtracted. The peak intensity value obtained via a Gaussian fit to the 8-T data shown in c is plotted as well. The solid line is a linear fit.

this PLCCO sample. Future experiments are needed to precisely map out the detailed field dependence of this field-induced AF order in PLCCO ($T_c = 24$ K), which would in turn allow a more complete assessment of the concomitant suppression of the resonance mode and the creation of static AF order under field.

To compare neutron measurements with the superconducting heat capacity anomaly, a small piece cut from one of the crystals (8) studied in our neutron measurements was used to measure the electronic specific heat under various field strengths (Fig. 1 b and c). Similar to previous work on optimally electron-doped $\text{Pr}_{1.85}\text{Ce}_{0.15}\text{CuO}_4$ (25), the entropy in PLCCO is almost conserved between the normal and superconducting states for $0 < T < T_c$ (see *SI Appendix*). The entropy conversion between 0 K and temperatures immediately above T_c suggests that the fluctuation effects crucial for obtaining the correct superconducting condensation energy in hole-doped materials (15, 16) are much

less important for optimally electron-doped cuprates (25). Using mean-field theory, we estimate the superconducting condensation energy for PLCCO, along with the upper critical field (H_{c2}) necessary for the complete suppression of the superconductivity [$H_{c2}(T = 0) \approx 7$ T], and the results are plotted in Fig. 1d. The physical quantity referred to here as the condensation energy is calculated in terms of the entropy loss measured at a given T and field strength H through the relation

$$U_c(T) = \int_T^{T_c+15\text{K}} [S_N(T') - S_{SC}(T')]dT'. \quad [1]$$

Using the specific-heat-determined upper critical field and the data from Figs. 2 and 3, we plotted schematically the behavior of $S(\mathbf{Q}, \omega)$ at $\mathbf{Q} = (1/2, 1/2, 0)$ in the fully superconducting ($H = 0$) versus the superconductivity-suppressed ($H > H_{c2}$) states (Fig. 1 e and f). The resonance is observed only in the superconducting state, and it disappears at high field, where the spectral weight losses at the resonance and quasi-elastic energies (see *SI Appendix*) are compensated in part by the intensity gain at the elastic AF position (Fig. 1f). This case is different from that of hole-doped $\text{La}_{2-x}\text{Sr}_x\text{CuO}_4$ (18, 19) and electron-doped $\text{Nd}_{1.85}\text{Ce}_{0.15}\text{CuO}_4$ (32).

Because the reduction of the resonance intensity with increasing field in PLCCO parallels the suppression of the superconducting condensation energy (Fig. 1d), it is tempting to think that magnetic excitations contribute a major part of the superconducting heat capacity anomaly and condensation energy (Fig. 1 b-d). For optimally hole-doped $\text{YBa}_2\text{Cu}_3\text{O}_{6.95}$, the change in the magnetic excitations between the normal and superconducting states was $\langle m^2 \rangle_{\text{res}} = 0.08 \pm 0.014 \mu_B^2/\text{Cu}$, and the condensation energy was $U_c = 1.5$ K/Cu, thus giving a ratio $\langle m^2 \rangle_{\text{res}}/U_c = 0.06 \pm 0.009 \mu_B^2/\text{K}$ (13). In PLCCO, the integrated moment of the resonance is a much weaker $\langle m^2 \rangle_{\text{res}} = 0.0035 \pm 0.0014 \mu_B^2/\text{Cu}$ (see *SI Appendix*); however, the condensation energy also has a much smaller value of $U_c = 0.0687$ K/Cu (Fig. 1c), rendering a similar ratio of $\langle m^2 \rangle_{\text{res}}/U_c = 0.05 \pm 0.02 \mu_B^2/\text{K}$. Although this estimation in itself does not prove that magnetic excitations contribute a major part of the condensation energy, it is clear that the resonance is intimately related to the electron pairing and superconductivity.

The surprising observation of a simple tradeoff in intensities with increasing field between the resonance associated with the superconducting phase and the AF order in the nonsuperconducting phase is consistent with Raman scattering results (22). These results suggest that the AF and superconducting phases compete with each other. However, it is unclear whether the AF ordered phase is associated with vortices (33) and, therefore, is microscopically phase-separated from the superconducting phase or is uniformly distributed throughout the sample as suggested by muon spin relaxation measurements (26). The remarkable parallel between the suppression of the resonance and condensation energy with increasing magnetic field also suggests that the mode is fundamentally connected to superconductivity and the entropy loss associated with the phase's formation. Finally, our experiments elucidate a direct transition from a pure superconducting state without residual static AF order to an AF ordered state without superconductivity. Such a transition is not expected in conventional superconductors and therefore can be used to test theories for high- T_c superconductors (20, 21, 33-35). Future absolute measurements of magnetic excitations over a wider energy and momentum space in the low-temperature superconducting and nonsuperconducting normal states should enable a more quantitative determination of the magnetic exchange energy contribution to the superconduct-

ing condensation energy and thus help identify the driving force for electron pairing and high- T_c superconductivity.

Materials and Methods

Our inelastic neutron scattering experiments on electron-doped PLCCO ($a = b = 3.98 \text{ \AA}$, $c = 12.27 \text{ \AA}$; space group: $I4/mmm$) were performed at the IN-8, IN22, and BT-9 thermal triple-axis spectrometers at the Institute Laue-Langevin and the National Institute of Standards and Technology Center for Neutron Research, respectively. Cold neutron data were collected on the V2 triple-axis spectrometer at the Hahn-Meitner Institute. Here we denote positions in momentum space using $\mathbf{Q} = (h, k, l)$ in reciprocal lattice units in which $\mathbf{Q} [\text{\AA}^{-1}] = (h \ 2\pi/a, k \ 2\pi/b, l \ 2\pi/c)$. The applied magnetic field was vertical, and the copper

oxygen layers of the compound were aligned either in the horizontal scattering plane or perpendicular to it.

We thank Eugene Demler, Hong Ding, and Ziqiang Wang for helpful discussions. The neutron scattering part of this work was supported in part by the U.S. National Science Foundation DMR-0453804. The PLCCO single crystal growth at the University of Tennessee was supported by U.S. Department of Energy Office of Basic Energy Science Grant DE-FG02-05ER46202. Oak Ridge National Laboratory was supported by U.S. Department of Energy Contract DE-AC05-00OR22725 through University of Tennessee/Battelle, LLC. The work at the Chinese Academy of Sciences Institute of Physics was supported by Natural Science Foundation of China, the Chinese Academy of Sciences project International Team on Superconductivity and Novel Electronic Materials and the Ministry of Science and Technology project (2006CB601000 and 2006CB92180).

1. Birgeneau RJ, Stock C, Tranquada JM, Yamada K (2006) *J Phys Soc Jpn* 75:111003.
2. Scalapino DJ (1995) *Phys Rep* 250:330–365.
3. Abanov A, Chubukov AV, Schmalian J (2001) *J Electron Spectrosc Relat Phenom* 117–118:129–151.
4. Rossat-Mignod J, Regnault LP, Vettier C, Bourges P, Burlet P, Bossy J, Henry JY, Lapertot G (1991) *Physica C* 185:86–92.
5. Mook HA, Yethiraj M, Aeppli G, Mason TE, Armstrong T (1993) *Phys Rev Lett* 70:3490–3493.
6. Dai P, Mook HA, Hunt RD, Doğan F (2001) *Phys Rev B* 63:054525.
7. Fong HF, Bourges P, Sidis Y, Regnault LP, Ivanov A, Gu GD, Koshizuka N, Keimer B (1999) *Nature* 398:588–591.
8. Wilson SD, Dai P, Li S, Chi S, Kang HJ, Lynn JW (2006) *Nature* 442:59–62.
9. Demler E, Zhang S-C (1998) *Nature* 396:733–735.
10. Chakravarty S, Kee H-Y (2000) *Phys Rev B* 61:14821–14824.
11. Dai P, Mook HA, Hayden SM, Aeppli G, Perring TG, Hunt RD, Dogan F (1999) *Science* 284:1344–1347.
12. Dai P, Mook HA, Aeppli G, Hayden SM, Doğan F (2000) *Nature* 406:965–968.
13. Woo H, Dai P, Hayden SM, Mook HA, Dahm T, Scalapino DJ, Perring TG, Dogan F (2006) *Nat Phys* 2:600–604.
14. Kee H-Y, Kivelson SA, Aeppli G (2002) *Phys Rev Lett* 88:257002.
15. Chakravarty S, Kee H-Y, Abrahams E (1999) *Phys Rev Lett* 82:2366.
16. Chakravarty S, Kee H-Y, Abrahams E (2003) *Phys Rev B* 67:100504.
17. Scalapino DJ, White SR (1998) *Phys Rev B* 58:8222–8224.
18. Lake B, Aeppli G, Clausen KN, McMorrow DF, Lefmann K, Hussey NE, Mangkorntong N, Nohara M, Takagi H, Mason TE, Schröder A (2001) *Science* 291:1759–1762.
19. Tranquada JM, Lee CH, Yamada K, Lee YS, Regnault LP, Rønnow HM (2004) *Phys Rev B* 69:174507.
20. Demler E, Sachdev S, Zhang Y (2001) *Phys Rev Lett* 87:067202.
21. Kivelson SA, Lee D-H, Fradkin E, Oganesyan V (2002) *Phys Rev B* 66:144516.
22. Machtoub LH, Keimer B, Yamada K (2005) *Phys Rev Lett* 94:107009.
23. Dagan Y, Qazilbash MM, Hill CP, Kulkarni VN, Greene RL (2004) *Phys Rev Lett* 92:167001.
24. Boothroyd AT, Doyle SM, Paul Mc KD, Osborn R (1992) *Phys Rev B* 45:10075–10086.
25. Balci H, Greene RL (2004) *Phys Rev B* 70:140508.
26. Kadono R, Ohishi K, Koda A, Saha SR, Higemoto W, Fujita M, Yamada K (2005) *J Phys Soc Jpn* 74:2806–2812.
27. Fujita M, Matsuda M, Katano S, Yamada K (2004) *Phys Rev Lett* 93:147003.
28. Kang HJ, Dai P, Mook HA, Argyriou DN, Sikolenko V, Lynn JW, Kurita Y, Komiya S, Ando Y (2005) *Phys Rev B* 71:214512.
29. Lake B, Rønnow HM, Christensen NB, Aeppli G, Lefmann K, McMorrow DF, Vorderwisch P, Smeibidl P, Mangkorntong N, Sasagawa T, Nohara M, *et al.* (2002) *Nature* 415:299–302.
30. Khaykovich B, Lee YS, Erwin RW, Lee SH, Wakimoto S, Thomas KJ, Kastner MA, Birgeneau RJ (2002) *Phys Rev B* 66:014528.
31. Khaykovich B, Wakimoto S, Birgeneau RJ, Kastner MA, Lee YS, Smeibidl P, Vorderwisch P, Yamada K (2005) *Phys Rev B* 71:220508(R).
32. Motoyama EM, Mang PK, Petitgrand D, Yu G, Vajk OP, Vishik IM, Greven M (2006) *Phys Rev Lett* 96:137002.
33. Demler E, Hanke W, Zhang S-C (2004) *Rev Mod Phys* 76:909–974.
34. Chakravarty S, Laughlin RB, Morr DK, Nayak C (2001) *Phys Rev B* 63:094503.
35. Lee PA, Nagaosa N, Wen X-G (2006) *Rev Mod Phys* 78:17–86.